

Reconstructed high-resolution forest dynamics and human impacts of the past 2300 years of the *Parc national de Mont-Orford*, southeastern Québec, Canada

The Holocene
1–14

© The Author(s) 2021



Article reuse guidelines:
sagepub.com/journals-permissions
DOI: 10.1177/0959683621994642
journals.sagepub.com/home/hol



Claire E. O'Neill Sanger,¹ Jeannine-Marie St-Jacques,¹ 
Matthew C. Peros² and Kayden Avery Schwartz¹

Abstract

We used a high-resolution lacustrine pollen record from Étang Fer-de-Lance (45°21'21.9"N, 72°13'35.3"W), southeastern Québec, Canada, together with microcharcoal, to infer forest dynamics and human impacts over the past 2300 years. The lake is located in the eastern sugar maple-basswood forest domain of the Northern Temperate Forest of eastern North America. We found that the pollen percentages and influxes of *Fagus grandifolia* (American beech) and *Tsuga canadensis* (eastern hemlock) significantly declined over the past 700 years. Over the last millennium, the pollen percentages and influxes of the *Picea* species (*P. glauca*, *P. mariana*, *P. rubens*) (white, black, and red spruce), and *Pinus strobus* (eastern white pine) significantly increased. We showed that these shifts in forest composition are being driven by changes in regional climate. In addition to the pollen percentage changes, the Medieval Climate Anomaly (AD 800–1300) appeared as increased pollen influxes and the Dark Ages Cold Period (AD 400–700) and Little Ice Age (AD 1400–1800) appeared as decreased pollen influxes. The signal for human modification of the landscape first appeared at ~AD 1550–1650 as increases in *Ambrosia* (ragweed) and Poaceae (grasses) from possible Indigenous agriculture. The signal of European settler landscape modification appeared at ~AD 1770 as the beginning of a steep, “classic” *Ambrosia* rise. It intensified over the subsequent 250 years as further increases in non-arboreal pollen taxa and early successional *Acer* (maple) species. Microcharcoal analysis showed that fire was a re-occurring event in the sugar maple-basswood domain, but had little impact on forest composition.

Keywords

high-resolution pollen analysis, Little Ice Age, Medieval Climate Anomaly, pre-Contact Indigenous agriculture, Québec, vegetation dynamics

Received 5 August 2020; revised manuscript accepted 3 January 2021

Introduction

Post-glacial vegetation records spanning the late Glacial Period and Holocene have been well documented throughout Québec (Hausmann et al., 2011; Houle et al., 2012; Lavoie and Richard, 2017, 2000; Mott, 1977; Muller and Richard, 2001; Muller et al., 2003; Richard, 1975, 1978, 1994). While these studies have led us to understand the migration of trees to lands newly exposed by the retreating Laurentide Ice Sheet and subsequent forest coarse-scale dynamics over the Holocene, the low resolution of many of these studies is insufficient to understand forest dynamics at shorter and more recent timescales, especially given the high amount of noise in pollen records (Lafontaine-Boyer and Gajewski, 2014). Given this, finer temporal- and spatial-scaled paleoenvironmental studies are needed in order to better understand forest dynamics over decadal to centennial periods (e.g. St-Jacques et al., 2008a, 2008b). The three existing high-resolution pollen research studies from southwestern and south-central Québec have proven effective in capturing vegetation dynamics and responses to short periods of climate variation, such as the Little Ice Age (LIA) (~AD 1400–1800) and the Medieval Climate Anomaly (MCA) (~AD 800–1300) (Houle et al., 2012; Lafontaine-Boyer and Gajewski, 2014; Paquette and Gajewski, 2013).

Pollen-climate transfer functions applied to sedimentary pollen records have allowed climate reconstructions over the entire Holocene (Kaufman et al., 2020). At a finer scale, high-resolution pollen analysis can also be used to reconstruct recent climate, particularly when done at sensitive ecotones (Shuman et al., 2018; St-Jacques et al., 2008a, 2008b, 2015). The synthesis paper of Marlon et al. (2017) showed that New England and southeastern Canada have undergone a general cooling trend over the past 2000 years (i.e. a warm first millennium AD, a cooler MCA and a yet colder LIA) using a wide variety of terrestrial and nearshore oceanic proxies. The hydroclimatic syntheses of Ladd et al. (2018), Marlon et al. (2017), and Shuman et al. (2018) found that

¹Department of Geography, Planning and Environment, Concordia University, Québec, Canada

²Department of Environment and Geography, Bishop's University, Québec, Canada

Corresponding author:

Jeannine-Marie St-Jacques, Department of Geography, Planning and Environment, Concordia University, 1455 Blvd. De Maisonneuve Ouest, 1255-45 Henry Hall Building, Sir George Williams Campus, Montréal, QC H3G 1M8, Québec, Canada.

Email: jeanninemarie.st-jacques@concordia.ca



Figure 1. Location of Étang Fer-de-Lance (yellow triangle) in the Parc national du Mont-Orford and in southeastern Québec (1) in upper-left inset. Also in upper-left inset are shown: (2) Lac Noir, (3) Lac Brulé, (4) Conroy Lake, (5) Basin Pond, (6) Clear Pond, (7) Wolf Lake, and (8) Sidney Bog. Red circle on the lower-right inset map shows the coring location.

northern New England experienced a general wetting trend over the last two millennia. There is a current debate as to how detectable the MCA and LIA are in pollen records from southern Québec; that is, whether they had a discernable effect on the forests of this region (Hausmann et al., 2011; Richard, 1994; Van Bellen and ClimHuNor Project Members, 2018, 2020), hence any new pollen study will be informative here.

Although forest fire is commonly thought to be a feature of western North American or boreal landscapes, fire is also a natural part of the northeastern deciduous forest (Carcaillet and Richard, 2000; Clark and Royall, 1996). Limited research using high-resolution microcharcoal from recent lake sediments to infer forest fires has been done in southwestern Québec and northern New England (e.g. Blarquez et al., 2018; Clark and Royall, 1996; Clifford and Booth, 2013; Lafontaine-Boyer and Gajewski, 2014; Paquette and Gajewski, 2013; Stager et al., 2016), but not in densely-populated southeastern Québec. There has also been limited research determining in situ forest fire dates using macrocharcoal from soils from two sites in the southern mixed forest of Québec (Payette et al., 2015, 2016). Given the many forest types of southern Québec (Ressources Naturelles Québec, 2003), there is a need for continuous high-resolution lacustrine paleo-fire studies from each forest type to better understand the natural fire-vegetation relationship, which can only be studied using paleo-methods because of modern fire suppression. A benefit of such studies would be that in densely-populated southern Québec, fire-risk assessments have incorporated little-to-no pre-historical data and little is known about long-term fire-climate relationships.

Our purpose was to investigate how forest composition changed in response to the changes in climate and human activities, and forest fires over the last two millennia using high-resolution pollen and

microcharcoal records from a small lake, *Étang Fer-de-Lance*, situated in southeastern Québec, Canada. We examined whether the forest composition changes were caused by regional climate changes by comparing reconstructed climate variables from our site to those from other nearby high-resolution climate proxy records. We assume that if the reconstructions are similar, then the vegetation changes are caused by regional climate change. This study produced paleo-environmental records in this region previously unstudied at high resolution, and helps determine how sensitive the local sugar-maple hardwood forests have been to climate change over the last two millennia. We also investigated the effects of historical land-use changes in the region on forest vegetation and the relationship between vegetation and fire from the eastern sugar maple-basswood domain (Ressources Naturelles Québec, 2003). This is a forest type from which no recent, high-resolution, lacustrine paleo-fire records previously existed.

Study area and methods

Study area

Étang Fer-de-Lance (45°21'21.9"N, 72°13'35.3"W) is a small 1 km long and 250 m wide lake which features a minerotrophic peatland situated in the *Parc national du Mont-Orford*, 20 km west of Sherbrooke in the Eastern Townships of Québec (Figure 1). The park is part of the Appalachian Mountain range in Québec and contains the peaks of *Mont-Orford* (maximum altitude of 853 m), *Pic de l'Ours* (740 m) and *Mont Chauve* (600 m) (Gauvin and Bouchard, 1983; Société des Établissements de Plein Air du Québec [SEPAQ], 2019). The Parc national du Mont-Orford covers a total area of 59.5 km². Étang Fer-de-Lance has a maximum depth of 3.9 m and the lake is at an elevation of 288 m and is situated between two streams, *Ruisseau*

des Hêtres and Ruisseau des Hourdes, in a valley bordered by the Pic de l'Ours and Mont Chauve. The small lake is only accessible by foot. Though little is known about the occupation of the area before European settlement, prior to the creation of the park in 1938, the area was predominantly used for forestry and agriculture (Gauvin and Bouchard, 1983; SEPAQ, 2019).

Currently, a stand of *Pinus strobus* L. (white pine) with some *Picea glauca* (Moench) Voss (white spruce) is located on the north shore of Étang Fer-de-Lance. *Pinus rigida* Mill. (pitch pine) also grows on the north shore, and there is a *Tsuga canadensis* (L.) Carrière (eastern hemlock) grove upslope. The south shore is dominated by *Thuja occidentalis* L. (eastern white cedar) and *T. canadensis*, while more inland, *Acer rubrum* L. (red maple), *Acer saccharum* Marsh. (sugar maple) and *Betula alleghaniensis* Britt. (yellow birch) dominate. In the park as a whole, mesic forests of low altitude are dominated by *A. saccharum*, while the summits have mixed forests of *Abies balsamea* L. (Mill.) (balsam fir), *Betula papyrifera* Marsh. (white birch), and *Picea rubens* Sarg. (red spruce) (Gauvin and Bouchard, 1983). Moist habitats are dominated by *T. canadensis* or *A. balsamea*.

The Mont-Orford region has an average annual temperature of 5.6°C and an average annual precipitation of 1142 mm (Government of Canada, 2019). It is situated within the eastern sugar maple-basswood domain of the hardwood forest subzone of Northern Temperate Forest between the colder eastern sugar maple-yellow birch domain (~50 km northeast) and the warmer sugar maple-bitternut hickory domain (~50 km southwest). Because of this proximity to these nearby ecotones and the altitudinal gradient, the park's forests should be sensitive to centennial-scale temperature change (Gauvin and Bouchard, 1983; Ressources Naturelles Québec, 2003; SEPAQ, 2019).

Field methods

Three sediment core drives were extracted from the deepest point near the center of Étang Fer-de-Lance (45°21'22.1"N, 72°13'35.1"W) in June 2018 from a floating platform. For the coring, we used a transparent tube fitted with a piston to capture the unconsolidated surface sediments (FDL2) and a Livingstone piston corer for the deeper, consolidated sediments (FDL-P2 and FDL-P3; Supplemental Figure 1). The drives collected using the Livingstone corer were sampled approximately 50 cm from those collected by the hollow tube to provide an overlap in the sedimentary sequence. The sediments at the sediment-water interface (SWI) were extruded vertically on-site into Ziploc bags with a sampling resolution of 1 cm. The core drives extracted with the Livingstone piston corer were immediately transferred into hard plastic tubing lined with plastic wrap and aluminum foil and left intact for analysis.

Chronology methods

Eleven ¹⁴C and 12 ²¹⁰Pb dates were obtained from plant macrofossils and surface sediment samples, respectively, throughout the core (Supplemental Figure 1). Radiocarbon analysis was performed on the plant macrofossils at the A.E. Lalonde AMS Laboratory (University of Ottawa), and the ¹⁴C dates were calibrated using OxCal v4.3 and the IntCal13 calibration curve for northern hemisphere terrestrial samples (Ramsey, 2009; Reimer et al., 2013). The ²¹⁰Pb dates were obtained from the first 40 cm of the surface core FDL2 and processed at Geotop (*Université du Québec à Montréal*). The constant rate of supply (CRS) model was used to interpret the ²¹⁰Pb depth profile (Ghaleb, 2009). The ¹⁴C and ²¹⁰Pb dates were used to produce an age-depth model using the R package Bacon (version 2.4.0), using Bayesian methods to reconstruct accumulation rates of sediments and ages were calculated to a 1 cm resolution throughout the depth of the core (Blaauw and Christen, 2011).

Loss-on-ignition analysis methods

Organic, carbonate and silicate content were estimated at 1 cm intervals along the core using loss-on-ignition (LOI) (Heiri et al., 2001). Samples were first dried at 105°C overnight and weighed, then heated at 550°C for 4 h and weighed to measure organic material, and then heated at 950°C for 2 h and weighed again to measure carbonate and silicate content. Porcelain lids were used through-out, and samples were cooled in a desiccator.

Pollen analysis methods

Samples of 1.23 cm³ of sediment were taken for pollen analysis at 2–4 cm intervals along the core, with the second millennium AD sampled at the higher rate. Each sample was spiked with one *Lycopodium* tablet (batch # 3862 from the University of Lund) to permit the calculation of pollen concentration (Benninghoff, 1962; Berglund, 1986; Bonny, 1972; Moore et al., 1991). Samples were treated with HCl, KOH, acetolysis, and HF in order to remove as much non-pollen components of the sediment as possible (Faegri and Iversen, 1989; LacCore, 2016). Pollen samples were stained using safranin and mounted in silicone oil on microscope slides (Faegri and Iversen, 1989). Pollen accumulation rates were calculated according to Berglund (1986) (p. 462).

High taxonomic resolution pollen counts were conducted with a minimum sum of 500 pollen grains from each sample. Pollen slides were counted at 400× or 800× using a Leica DM 2500 LED microscope at the *Climatology, Hydrology and Paleo-Environmental Laboratory* at Concordia University. Regional pollen guides (Bassett et al., 1978; McAndrews et al., 1973; Richard, 1970) were used as references. *Pinus* (pine) pollen grains were identified as *Pinus Haploxylon* or *Pinus Diploxylon* to distinguish between *Pinus strobus* (Haploxylon) and other Diploxylon species of *Pinus* possibly present, that is, *Pinus rigida*, *Pinus resinosa* Ait. (red pine), and *Pinus banksiana* Lamb. (jack pine) (McAndrews et al., 1973; Richard, 1970). *Betula alleghaniensis*, *Betula papyrifera* (paper birch), and *Betula populifolia* (Marsh.) (gray birch) are all present in the Mont-Orford region (Gauvin and Bouchard, 1983), and they have pollen grains of overlapping sizes (Richard, 1970), hence *Betula* pollen grains were identified to genus level.

Constrained Clustering with Incremental Sum of Squares (CONISS) was used to separate the pollen stratigraphy into distinct zones (Juggins, 2019). Principal Component Analysis (PCA) ordination using the correlation matrix was used to confirm the CONISS pollen zones and to calculate the principal components to better understand the temporal variation of the pollen record. These analyses were done on the taxa with at least one occurrence ≥5%.

Changes in pollen percentages and influxes of ecologically key taxa between pollen zones were detected using Welch two-sample two-sided *t*-tests assuming unequal variances after verification that the data were normally distributed and no significant autocorrelation was present. If significant lag-1 autocorrelation was present but the data was normally distributed, adjusted *t*-tests were used with the effective sample sizes adjusted for autocorrelation (Santer et al., 2000). Otherwise, lower-power Wilcoxon rank sum tests were used. A significance level of *p* = 0.1 was used.

Charcoal methods

Fire occurrence intervals were based on analysis of sedimentary microcharcoal. Contiguous samples of 1 cm³ were analyzed for their charcoal content along the entire core. Samples were soaked ~12 h in sodium hexametaphosphate (Na₆PO₃)₆ and then ~12 h in aqueous 6% sodium hypochlorite (NaClO) to deflocculate and bleach the sediment. Charcoal particles were sieved with a 150 μm Nitex® mesh, then counted and measured using a Leica M80 stereoscope paired with an image analysis system (WinSeedle®, Regent Instruments, Québec, Québec). We used charcoal area

because charcoal abundance could be subject to fragmentation during preparation, causing errors. Fire occurrence reconstruction was done using CharAnalysis 0.9 software in Matlab© using a 400-year window width, a robust LOWESS smoother, and a locally-defined 95% threshold based on a Gaussian mixed model (Higuera, 2009; Higuera et al., 2009).

Climate reconstruction methods

To provide evidence that the shifts in vegetational composition were driven by regional climate changes, we converted the high-resolution pollen relative abundance data into temperature and precipitation values and compared the climate signal from this site with that from other sites in the region. We assume that if the reconstructions are similar, then the vegetation changes are caused by regional climate change. We reconstructed past climate, that is, summer (JJA) average temperature and annual precipitation, using the modern analog technique (MAT). For the pollen-climate calibration set, we used version 1.72 of Whitmore et al. (2005), together with the squared-chord distance metric (Overpeck et al., 1985). For the calculations, we used C2 software (Juggins, 2007). A total pollen sum of 50 arboreal and terrestrial herbaceous pollen taxa was used. Given the taxonomic decisions of the earlier researchers whose work forms the pollen-climate training set, we had to merge the *Picea* taxa. Modern pollen data spanning 64° and 80°W longitude and 41° and 49°N latitude were extracted as candidates for modern analogs, resulting in 620 sites in the calibration set. The average of the first three analogs was used to compute the reconstructed climate variables. The fifth percentile of the distribution of pair-wise dissimilarities from the training-set samples was used as the definition of close analogs (Simpson, 2012). We compared our reconstructions to other high-resolution and well-dated sedimentary reconstructions from within a 350 km radius to examine regional past climate patterns. We defined high-sampling resolution analysis as at least four proxy samples per century, and well-dated to mean varved sediments or at least eight ¹⁴C dates per 2000 years. We used MAT to be able to compare our results to other nearby high-resolution climate reconstructions using this method (i.e. Lafontaine-Boyer and Gajewski, 2014; Paquette and Gajewski, 2013).

Results

Sediment cores, age-depth model construction, and LOI analysis

The three sediment core drives span 0–247 cm below the SWI (Supplemental Figure 1). The first drive, FDL2, is 76 cm long. The deeper second piston core, FDL_P2, is 101 cm long and spans 50–151 cm below the SWI, while the third and deepest piston core, FDL_P3, has a length of 96 cm and spans 151–247 cm. There is a 26 cm overlap between FDL2 and FDL_P2. The alignment of FDL2 and FDL_P2 was confirmed by pollen counts from both cores within the overlap; however, the analysis only uses pollen counts from FDL2 in the section of overlap. The three aligned sediment core drives were combined to form a composite core and will be referred to as “the core” hereafter. The sediments in the core are uniformly dark brown in color and have an organic gyttja consistency throughout.

Of the 14 sediment samples submitted for ²¹⁰Pb dating, 12 yielded measurable dates (Supplemental Table 1). The ²¹⁰Pb samples dated from AD 1880 to 2018, establishing the chronology of the first 40 cm of the core. The ²¹⁰Pb activity results reflect the ideal case where ²¹⁰Pb activity declines exponentially with increasing depth due to radioactive decay (Ghaleb, 2009; Sorgente et al., 1999), as it decreases from 35.404 ± 2.297 dpm/g at 2.5 cm to 1.627 ± 0.138 dpm/g at 50 cm below the SWI, with the exception of the first sample at 0.5 cm (Supplemental Figure 2). The outlier

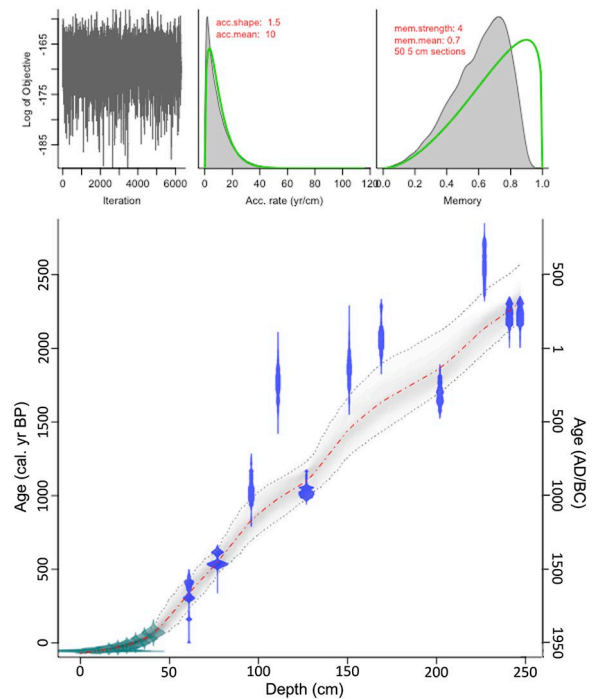


Figure 2. Age-depth model for the Étang Fer-de-Lance core using the R package Bacon. The age-depth model includes ²¹⁰Pb (green) and ¹⁴C (blue) dates. The central red dotted line is the best fit model and the outer gray dotted lines denote the 95% confidence interval.

²¹⁰Pb activity of the initial sample is likely due to mixing with water and dilution of the surface sediment sample.

The age-depth model spans ~365 BC to ~AD 2018 (Figure 2 and Supplemental Table 2). Plotted in gray are the mean 95% confidence intervals which have a mean of 290 years, ranging from a minimum of 4 years (at 1.5–2 cm) to a maximum of 470 years (at 170 cm). All but one of the 11 ¹⁴C dates overlap with the Bayesian age-depth model’s 95% confidence range, however, there is variability in the calibrated age ranges below 110 cm. The source of this variability is unclear but may represent the effects of bioturbation or wind-induced mixing of the sediments. In addition, several dates were made on wood which can influence radiocarbon chronologies through the “old wood” effect (Oswald et al., 2005). In the case of Étang Fer-de-Lance, however, we note that two of the wood dates (76–77 cm and 126–127 cm) fall directly within the 95% confidence interval of the age model, suggesting that these are unaffected by either vertical mixing of the sediments or the “old wood” effect. We have thus decided to retain all ¹⁴C dates for the age model, although note that the chronology below 110 cm (i.e. older than approximately 1000 cal yr BP) is less reliable than the chronology before this time.

Loss-on-ignition analysis results are relatively uninformative (Supplemental Figure 3). Organic material, carbonate and silicates are by-and-large constant through-out the core at 45.8%, 7.5%, and 46.7%, respectively.

Pollen results

In total, 102 samples were counted from the core, yielding an average sample interval of 23 years. Pollen assemblages at Étang Fer-de-Lance show that its forest has been dominated over the last 2300 years by *Betula* spp., *T. canadensis*, *Fagus grandifolia* Ehrh. (American beech), *Picea* spp. (*Picea glauca*, *Picea mariana* (Mill.) Britton, Sterns & Poggenburg (black spruce), and/or *Picea rubens*) (summary diagram in Figure 3 and full pollen diagram in Supplemental Figure 4). CONISS and PCA were used to divide

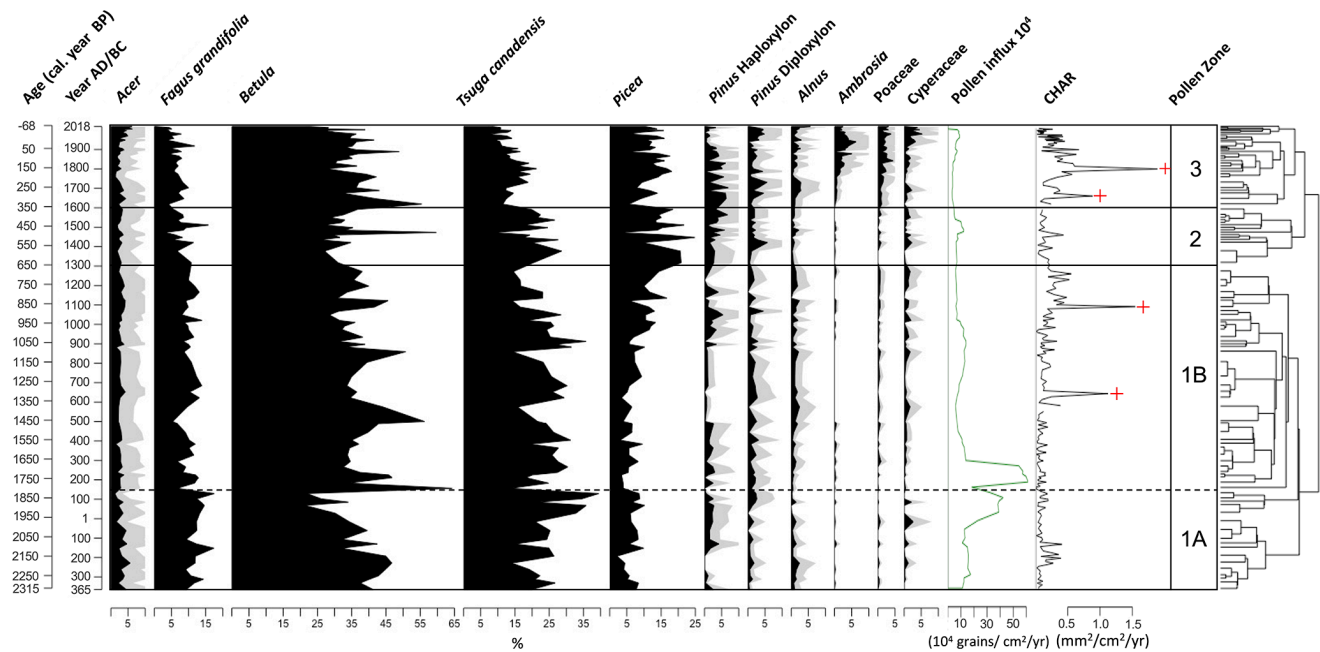


Figure 3. Pollen percentage diagram for principal taxa from Étang Fer-de-Lance, Québec. Shown are pollen percentages of main taxa (total pollen sum $>5\%$ at least once in the record). Light gray areas show an exaggeration of $3\times$. The 5-point moving average of pollen influx (10^4 grains/cm²/year), pollen concentration (10^4 grains/cm³), and charcoal accumulation rate (CHAR) (mm²/cm²/year) are plotted as well. Significant charcoal peaks indicated with a cross.

the pollen percentage diagram of the taxa with at least one occurrence $\geq 5\%$ into three pollen zones (Figures 3 and 4). CONISS and PCA on the full pollen assemblage of 50 taxa gave identical results (Supplemental Figure 4, Supplemental Text 1).

Between ~ 365 BC and \sim AD 1300 (Pollen Zone 1, 85.5–247.5 cm), concurrent with the first millennium AD and the MCA, *Betula* spp. and *T. canadensis* maintained high percentages and influxes (Figure 3 and Supplemental Figure 5). *Fagus grandifolia* has significantly higher average percentage and influx in Pollen Zone 1 (11.0% and 2.0×10^4 grains/cm²/year) than compared to the subsequent 700 years (6.9% and 4.4×10^3 grains/cm²/year) (Table 1). *Acer* spp. (*Acer saccharum*, *Acer rubrum*, *Acer pensylvanicum* L. (striped maple), *Acer spicatum* Lam. (mountain maple), *Acer saccharinum* L. (silver maple), and *Acer negundo* L. (Manitoba maple)) has an average abundance of 3% and an average influx of 5.0×10^3 grains/cm²/year throughout Pollen Zone 1. Percent *Picea* spp. increased over the course of the first millennium AD, beginning at \sim AD 900, rising from a low of 2% to a peak of 17%. Also beginning at \sim AD 900, *Pinus Haploxylon* percentage began an increase which continued into the second millennium. However, influx shows that these two conifer taxa are reasonably productive in pollen throughout Zone 1 except during the Dark Ages Cold Period (AD 400–700). *Alnus* spp. (*Alnus crispa* (Cryander ex Ait.) Turr. ex Ait. and *Alnus incana* subsp. *rugosa* (Du Roi) R.T. Clausen), Poaceae (grasses), and Cyperaceae (sedges) have low and constant percentages and influxes, while *Ambrosia*-type pollen is barely present throughout Pollen Zone 1. Total pollen influx is relatively high throughout Pollen Zone 1 (an average of 2.3×10^5 grains/cm²/year) with two major peaks at \sim AD 130 and \sim AD 270 (Figure 3). There is however a dip in total pollen influx and in the influxes of most arboreal taxa during AD 400–700 (Supplemental Figure 5).

Both CONISS and PCA divide Pollen Zone 1 into subzones 1A and 1B at \sim AD 130. The visual demarcation between these two pollen subzones is subtle but *F. grandifolia* percentage is higher in subzone 1A and declines in subzone 1B, while *Picea* spp. percentage is lower in subzone 1A and higher in subzone 1B. As well, a sharp decline in *Betula* percentage occurs at and prior

to \sim AD 130 due to an increase in *T. canadensis* percentage and influx (Figure 3 and Supplemental Figure 5).

Between \sim AD 1300 and 1600 (Pollen Zone 2; 62.5–82.5 cm), concurrent with the early LIA, the average *Betula* species percentage (33.2%) and influx (2.7×10^4 grains/cm²/year) significantly decrease compared to Pollen Zone 1 (37.4% and 6.1×10^4 grains/cm²/year) (Figure 3 and Table 1). Mean percentages of *T. canadensis* and *F. grandifolia* also significantly decline from Pollen Zone 1 (23.9% and 11.0%, respectively) in comparison to Pollen Zone 2 (21.1% and 8.2%), as do their influxes (5.0×10^4 grains/cm²/year and 2.0×10^4 grains/cm²/year, respectively, in Zone 1 vs 1.2×10^4 grains/cm²/year and 6.6×10^3 grains/cm²/year in Zone 2). The *Acer* species decline to an average abundance of 2.7%, and their mean influx declines to 2.1×10^3 grains/cm²/year. Percent *Picea* spp. (16.0%) increases significantly between \sim AD 1300 and 1600, relative to its prior mean percentage in Pollen Zone 1 (7.6%), as does its influx (1.3×10^4 grains/cm²/year vs 7.9×10^3 grains/cm²/year). Percent *Pinus Haploxylon* significantly increases gradually throughout Pollen Zone 2 with a mean of 3.3%, relative to its previous mean of 1.5% in Zone 1, as well as its influx. Contrarily, *Pinus Diploxylon* percentage does not increase significantly between Pollen Zone 1 (1.4%) and Pollen Zone 2 (1.9%), and neither does its influx. *Alnus* spp., Poaceae and Cyperaceae continue to have low percentages and influxes throughout Pollen Zone 2, and *Ambrosia*-type percentages and influx remains negligible, but sporadically present. The total pollen influx is significantly lower in Pollen Zone 2 (7.9×10^4 grains/cm²/year) relative to Zone 1 (2.3×10^5 grains/cm²/year).

Between \sim AD 1600 and 2018 (Pollen Zone 3; 0–60.5 cm), beginning during the late LIA and early European settlement, there is a striking increase in non-arboreal pollen (NAP) as *Ambrosia*-type pollen, Poaceae and Cyperaceae percentages and influxes begin to increase at the beginning of Pollen Zone 3 (Figure 3 and Supplemental Figure 5). The *Ambrosia* rise is characterized by two distinct periods of increase. An early *Ambrosia* rise beginning at \sim AD 1650 (58.5 cm) and lasting until \sim AD 1760 (50.5 cm) is comprised of relatively stable percentages ranging from 0.5% to 0.8%

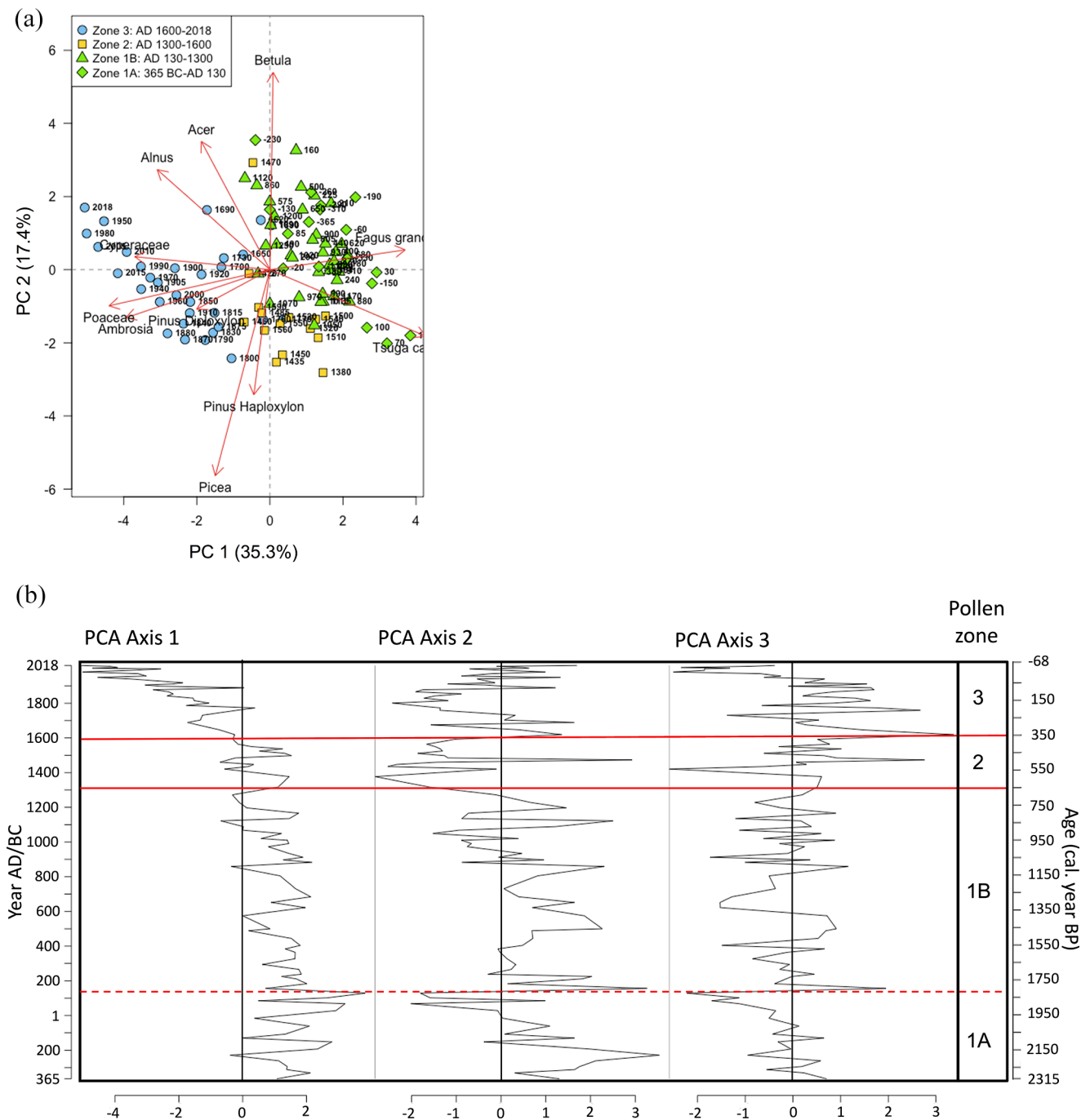


Figure 4. (a) PCA biplot of Étang Fer-de-Lance pollen percentages with symbols denoting the pollen zones of the observations. Negative numbers denote years BC, (b) Étang Fer-de-Lance PCA sample scores (unsmoothed) for the first three principal components (~365 BC–AD 2018). Pollen zones and subzones shown with red lines.

and similarly stable influxes. A subsequent more “classic” steep *Ambrosia* rise (e.g. Brugam, 1978; Grimm, 1983, 2001) begins at ~AD 1770 (49.5 cm) and increases from 1.4% to 6.3% by ~AD 1940, after which it declines slightly. *Fagus grandifolia* percentages and influxes significantly decline from means of 8.2% and 6.6×10^3 grains/cm²/year in Pollen Zone 2 to means of 6.2% and 3.4×10^3 grains/cm²/year in Pollen Zone 3 (Table 1), but influx increases slightly in the last century. *Acer* percentages and influx increase throughout Pollen Zone 3, particularly over the last 100 years. This increase is primarily due to an increase in *Acer rubrum* (Supplemental Figure 4). *Quercus* percentages also increase during the most recent 150 years (Supplemental Figure 4).

Tsuga canadensis percentages and influx significantly decline further to 13.5% and 7.2×10^3 grains/cm²/year. *Tsuga canadensis* and *Picea* spp. percentages initially decline in Pollen Zone 3, then increase ~AD 1800 and then gradually decline, but influx shows that they are slightly increasing over the most recent century. *Pinus Haploxylon* maintains relatively high percentages from the 1600s until ~AD 1870 when it declines until present day. *Alnus* percentage increases beginning in the early 1800s and peaks at 5.6% in the present, similarly for its influx. Total pollen and *Betula* influxes dip during the late LIA, ~AD 1600–1800 (Supplemental Figure 5).

PCA was used to uncover the main patterns of pollen variation (Figure 4 and Supplemental Table 3). The first three PCA axes

Table 1. Comparisons of pollen percentages and influxes between pollen zones of Étang Fer-de-Lance.

Taxon	Change in % mean	t-statistic (%)	p-Value (%)	df (%)	Change in influx mean	p-Value (influx)
Differences between Pollen Zone 1 and combined Pollen Zones 2 and 3						
<i>Fagus grandifolia</i>	↓	8.14	1.5×10^{-12}	95.0	↓	2.6×10^{-12}
Differences between Pollen Zone 1 and Pollen Zone 2						
<i>Betula</i> spp.	↓	1.86	0.08	21.3	↓	0.002
<i>Tsuga canadensis</i>	↓	1.92	0.07	27.4	↓	0.01
<i>F. grandifolia</i>	↓	3.26	0.004	19.3	↓	0.0003
<i>Picea</i> spp. ¹	↑	-5.26	0.0001	13.9	↑	0.03
<i>Pinus</i> Haploxyton	↑	-3.97	0.0008	19.2	↑	0.05
<i>Pinus</i> Diploxyton	N.S. ↑	-1.30	0.21	18.7	N.S. ↓	0.21
Total pollen influx	N.A.	N.A.	N.A.	N.A.	↓	0.006
Differences between Pollen Zone 2 and Pollen Zone 3						
<i>T. canadensis</i> ¹	↓	4.85	0.0003	13.0	↓	9.6×10^{-6}
<i>F. grandifolia</i>	↓	2.30	0.03	21.2	↓	0.001

Regular t-tests were used if the normality assumption was met and no autocorrelation present. If autocorrelation was present but the data was normal, a t-test adjusted for autocorrelation was used. Otherwise a Wilcoxon rank sum test was used. Wilcoxon tests were used for all influxes, because of strong non-normality. A significance level of $p=0.1$ was used. Non-significance denoted by N.S. Not applicable denoted by N.A.

¹t-test adjusted for autocorrelation.

explain 63.9% of the total pollen variation. PCA Axis 1 explains 35.3% of the pollen variation and is defined by late-successional *T. canadensis*, *F. grandifolia* (highest positive first axis species scores), and the disturbance indicator taxa: Poaceae, *Ambrosia*-type pollen, Cyperaceae, and *Alnus* spp. (lowest negative first axis species scores). PCA Axis 2 explains 17.4% of the pollen variation and is defined by the deciduous pollen of *Betula* spp. and *Acer* spp. (highest positive second axis species scores), and the coniferous pollen of *Picea* and *Pinus* Haploxyton (lowest negative second axis species scores). PCA Axis 3 explains 11.2% of the pollen variation and is defined by *Betula* spp. and *Pinus* Haploxyton (highest positive third axis species scores) and *Pinus* Diploxyton, *Acer* spp., and Cyperaceae (lowest negative third axis species scores). The eigenvalue scree plot (not shown) shows that subsequent PCA axes are not important. The pollen zonation (Figure 4) is based on this PCA ordination and CONISS (Figures 3 and 4), with the demarcation between Pollen Zones 2 and 3 defined by PCA Component 1, and the demarcation between Pollen Zones 1 and 2 defined by PCA Component 2. The sample scores on PCA axes 1 and 2 show a clean separation of the samples from Pollen Zones 1, 2 and 3 (Figure 4(a)). A PCA using the covariance matrix with a square root transform on the percentages of the taxa with abundances $\geq 5\%$ gave similar results, as did a PCA using the correlation matrix on all 50 taxa.

Charcoal analysis results

Charcoal particles were present throughout the entire core, showing that fire has long been present in the Mont-Orford forest landscape (Figure 3). The charcoal accumulation rate (CHAR) record increases during the Human-modified Period (Pollen Zone 3). The decomposition of the CHAR record into local fires (i.e. within 1 km of the pond (Higuera et al., 2009)) and background charcoal (from washed in old charcoal or from non-local fires) shows that significant local fires occurred at ~AD 645, ~AD 1090, ~AD 1660, and ~AD 1800. Assuming that significant fire peaks prior to ~AD 1760 (the beginning of regional European settlement) are naturally ignited fires, this produces a mean natural fire return interval of 515 years for this forest type in the region.

Climate reconstructions

The reconstructed summer temperature shows a warm first millennium AD, a slightly cooler MCA, and a distinct cold LIA

(Figure 5). The reconstructed warm first millennium AD spans ~365 BC to ~AD 950 with summer temperatures almost always above the pre-1900 average of 16.8°C, the slightly cooler MCA spans ~AD 950–1420 with summer temperatures oscillating above and below average, and the distinct cold LIA spans ~AD 1435–1800 with summer temperatures almost consistently below average. The reconstructed annual precipitation shows a gradually wetter climate from ~AD 700, with a mean annual precipitation of 1016 mm during the first millennium AD, a mean of 1062 mm in the MCA, a mean of 1084 mm in the LIA, and a mean of 1109 mm in the 1800s (Figure 5). Reconstructed JJA precipitation shows very similar results (not shown). Post-1900, the climate reconstructions become unreliable due to well-documented human-caused landscape modification. Analog matchings between the down-core samples and the training set are close, with only four samples having a minimum distance greater than that of 5% of the training set (22.9). Of these four poor analog samples (out of 102), two were from the most recent three decades and two from the early first millennium AD. The training set when run on itself using leave-one-out cross-validation had a $R^2=0.79$ and a root mean squared error of prediction $RMSEP=0.87^\circ\text{C}$ for JJA mean temperature, and a $R^2=0.49$ and $RMSEP=1112$ mm for annual precipitation. Analysis using a calibration set spanning 50° and 100°W longitude and 20° and 50°N latitude gave similar results.

Discussion

Vegetation history

Our results highlight the dominance of the mixed hardwood forest in the Mont-Orford region over the last 2300 years. While the pollen percentages of the major taxa remained relatively unchanged over the first 1600 years of the record, the pollen zones identify subsequent key vegetation changes tied to climatic and human events. Our record captures a clear increase in sub-dominant *Picea* spp. and *Pinus* Haploxyton relative abundances and influxes beginning in the late first millennium AD and a decrease in the relative abundances and influxes of the sub-dominant *F. grandifolia* and *T. canadensis* over the last 700 years.

Our pollen record captures a relatively unchanging first millennium AD for the percentages of most taxa, with dominant *Betula* spp., *T. canadensis*, and *F. grandifolia* (Figure 3). Regional *Betula* species include *B. alleghaniensis*, *B. papyrifera*, and *B.*

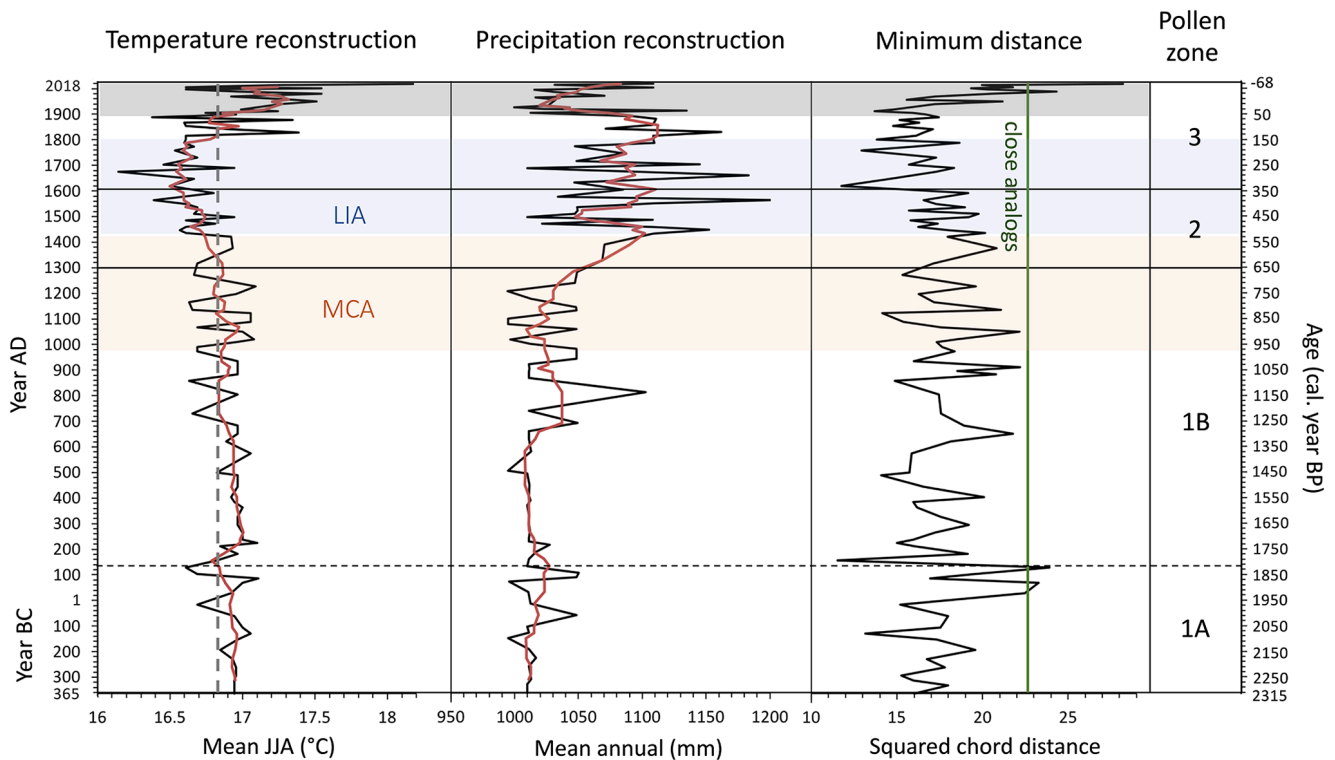


Figure 5. Reconstructed summer (JJA) temperature and mean annual precipitation for Étang Fer-de-Lance, Québec, using the modern analog technique (MAT), together with minimum squared chord distance for the closest analog. The gray dashed vertical line denotes 16.8°C – the mean pre-1900 temperature. The red lines are 5-point smoothers. Samples with a minimum squared chord distance of less than 22.9 are considered to have close analogs (green vertical line).

populifolia (Gauvin and Bouchard, 1983) and all could possibly have been present throughout the first millennium. While there are some changes in the various taxa percentages in the first millennium AD, these changes are smaller than the changes of the second millennium. The general stability of the first millennium AD for the pollen taxa percentages in Étang Fer-de-Lance is supported by other southern Québec studies that also found relatively unchanging first millennia AD (Houle et al., 2012; Lafontaine-Boyer and Gajewski, 2014). From Lac Clair, southcentral Québec, Houle et al. (2012), in their 1800-year-long record, found that main tree taxa percentages were less variable prior to AD 1500. A 1400-year-long record from Lac Brulé, southwestern Québec, similarly found little variation in pollen percentages until the early second millennium (Lafontaine-Boyer and Gajewski, 2014).

While we observe little change in pollen percentages during the first millennium AD at Étang Fer-de-Lance, prior to AD 400, total pollen influx and deciduous taxa pollen influx were higher (Figure 3 and Supplemental Figure 5) showing increased forest biomass production caused by warmer temperatures in the early first millennium (Grochoczek et al., 2019). These pollen influx rates are characteristic of hardwood-dominated mixed forest (Davis et al., 1975). The sharp spikes in pollen influx rates at AD 130 and AD 270 also appear in the pollen concentrations (Figure 3), suggesting pollen focusing during deposition and/or problems with the age-depth model and should be discounted. Total pollen influx and individual pollen taxa influx declined ~AD 400–700 (Figure 3 and Supplemental Figure 5), coincident with the Dark Ages Cold Period (Helama et al., 2017). This period frequently appears as a cold and wet period in northern Québec (e.g. Loisel and Garneau, 2010). The MCA shows most clearly as an increase in pollen influx and productivity during AD 800–1300 for *Acer* spp., *F. grandifolia*, *Betula* spp., *T. canadensis*, *Picea*, *Pinus* Haploxylon, and *Alnus* after their declines during the Dark Ages Cold Period.

After earlier low percentages of *Picea* spp. and *Pinus* Haploxylon, we see their rise beginning around ~AD 900, which persists throughout the second millennium (Figure 3). Pollen influxes (Supplemental Figure 5) shows that the rises in *Picea* and *Pinus* Haploxylon percentages are due to both increases in their influxes and declines in *Betula*, *Fagus*, and *Tsuga* influxes. This rise is consistent with studies in adjacent Maine which also found a *Picea* relative abundance and influx resurgence over the past 1000 years (Davis et al., 1975; Gajewski, 1987; Gajewski et al., 1987; Lindbladh et al., 2003; Nolan, 2019; Schauflier and Jacobson, 2002). In upstate New York and Vermont, the *Picea* increase occurs earlier still from early first millennium AD to AD 700 (Gajewski, 1987; Gajewski et al., 1987; Grochoczek et al., 2019; Oswald et al., 2018). In southwestern and southcentral Québec, the rise was found to be a little later – ~AD 1300 (Houle et al., 2012; Lafontaine-Boyer and Gajewski, 2014; Paquette and Gajewski, 2013). Although *Picea* were some of the first trees to have recolonized North American landscapes following the retreat of the Laurentide Ice Sheet, this recent northward increase of *Picea* follows an early-to-mid Holocene decline attributed to unfavorable climate characterized by high seasonality (Lindbladh et al., 2003). The *Picea* spp. increase beginning in the first millennium AD is in response to the general regional cooling (see below) due to orbital forcing and decreasing of seasonality (Marlon et al., 2017; Ruddiman, 2008). It is speculated that the higher Appalachian and Adirondack Mountains and colder and moister coastal areas served as refugia for *Picea* species in southern Québec and New England during the unfavorable growing conditions of the mid-Holocene (Lindbladh et al., 2003; Schauflier and Jacobson, 2002).

Unlike the regional increase in *Picea* percentage and influx, changes in *Pinus* are more heterogenous through time and space. *Pinus* Haploxylon percentage and influx (here *P. strobus*) significantly increased at Étang Fer-de-Lance ~AD 1300. The high-resolution Knob Hill Pond core from northern Vermont also shows

an increase in *P. strobus* percentage ~AD 1200 (Oswald et al., 2018). Lafontaine-Boyer and Gajewski (2014) and Paquette and Gajewski (2013) also observed an increase in this species' percentage and influx at Lacs Noir and Brulé, but at AD 1500. However, some nearby higher-resolution sites show no increase (i.e. Lac Clair) or declines (i.e. Mont Shefford; Richard, 1978). *Pinus* Diploxylon percentage and influx (i.e. *P. resinosa*, *P. rigida*, *P. banksiana*) show no significant change at this time at Étang Fer-de-Lance also.

The increase of *Picea* and *P. strobus* is accompanied by declines in other dominant taxa. Both *F. grandifolia* and *T. canadensis* percentages and influxes further declined beginning ~AD 1300 and continued to decline until present. The *F. grandifolia* and *T. canadensis* declines are found in other studies from northeastern North America and are attributed to the LIA and general regional cooling (Campbell and McAndrews, 1993; Gajewski, 1987; Grochoccki et al., 2019; Lavoie et al., 2013; Muller et al., 2003; Oswald et al., 2018; Pellerin et al., 2007). Our findings match results from southwestern Québec that found higher *F. grandifolia* and *T. canadensis* pollen percentages and accumulation rates in the first millennium AD, which then significantly declined in the mid-second millennium AD and have not returned to previous peaks (Lafontaine-Boyer and Gajewski, 2014; Paquette and Gajewski, 2013). At varved Lac Brulé, *F. grandifolia* and *T. canadensis* rapidly decline at AD 1375, while at varved Lac Noir, the abrupt changes began AD 1550. This decrease in the sub-dominant *F. grandifolia* and *T. canadensis* pollen and an increase in more boreal *Pinus*, *Picea*, and *Abies* pollen, suggests that there was a relatively rapid transition between a warmer MCA and a cooler LIA in southern Québec, which had a definite effect on the vegetation (Paquette and Gajewski, 2013).

Except for the above studies, much of the previous Québec pollen work has been low-resolution whole Holocene forest composition reconstructions (Lavoie and Richard, 2000; Muller and Richard, 2001; Richard, 1975, 1978, 1994). While yielding illuminating results for the whole Holocene, the resolutions of these studies are unable to easily capture the response of the vegetation to the LIA and MCA. Indeed, there is a debate as to whether it is even possible to discern the vegetation's response to the LIA and MCA in southern Québec pollen records (e.g. Hausmann et al., 2011; Richard, 1994; Van Bellen and ClimHuNor Project Members, 2018, 2020). By filling the lack of high-resolution pollen records in southeastern Québec, our findings help clarify the presence of a distinct early LIA and a MCA that previous low-resolution cores had difficulty detecting.

Ambrosia rises and the Human-modified Period

***Ambrosia* rises.** The Human-modified Period begins in ~AD 1600 (Pollen Zone 3) with the beginning of increases in shade-intolerant and disturbance-characteristic taxa, which has likely overshadowed the vegetative response to the late LIA. Étang Fer-de-Lance exhibits an unusual *Ambrosia* rise occurring in two steps and captures signs of possible Indigenous agriculture in the broader Mont-Orford region prior to European settlement in the late 1700's after the American Revolution. Our pollen record captures an initial early rise in *Ambrosia* beginning ~AD 1650 and then a second, more abrupt, classic *Ambrosia* rise (e.g. Brugam, 1978; Grimm, 1983, 2001) beginning ~AD 1770 and peaking in ~AD 1940. The *Ambrosia* initial rise is accompanied by an earlier Poaceae rise beginning ~AD 1550, which suggests increasing open spaces in the forest canopy of the pollenshed and could be due to increased land clearance for Indigenous crops. Stager et al. (2016) found increased erosion in Wolf Lake in Adirondack Park, New York, in the late 1600s and early 1700s which they also attributed to Indigenous agriculture (Figure 1). Several Montréal lowlands sites of Muller and Richard (2001) also show similar

early *Ambrosia* and Poaceae rises, but given their lower resolution and dating control this is less certain.

What could have been the cause of this early Poaceae/*Ambrosia* rise in ~AD 1550–1650, a time frame that suggests Indigenous agriculture rather than European? First of all, there could be dating issues with the Étang Fer-de-Lance core which has an estimated error of ± 80 years here. Montréal was founded in AD 1642 on the site of St-Lawrence Iroquoian Hochelaga (Tremblay, 2006), but remained small for many years. However, given dating error and noise in Poaceae abundance, perhaps this early rise is just a faint pollen signal of Montréal (located 105 km away) and its slowly increasing population, land clearance and farms (Dechêne, 1992).

Alternatively, the early Poaceae/*Ambrosia* rise could be due to Indigenous agriculture. In the late prehistorical and early historical periods, the region surrounding Mont Orford was controlled by the Missisquoi Abenaki (Calloway, 1994; Haviland and Power, 1994; Pendergast, 1989). The Missisquoi Abenakis, located on the eastern shores of Lake Champlain, obtained a portion of their diet from maize-based agriculture (Calloway, 1994). In AD 1534, Jacques Cartier reported that the St-Lawrence Iroquoians were in control of the island of Montréal and growing maize for their primary sustenance (Tremblay, 2006). Well known for their extensive crops of maize, beans and squash, the St-Lawrence Iroquois and the Haudenosaunee cleared forest for large fields (Haudenosaunee Confederacy, 2020; Tremblay, 2006). By AD 1609 when Samuel Champlain visited the island of Montréal, the St-Lawrence Iroquois were gone. Based on conversations with his local guides, Champlain estimated that intense warfare began ~AD 1570, leading to the vanishing of the St-Lawrence Iroquois from the St-Lawrence Valley (Calloway, 1994). Refugee groups may have been absorbed by the Missisquoi Abenakis (in northern Vermont/southern Québec), Huronia (in southern Ontario) or the Haudenosaunee Confederacy (in central New York) (Haviland and Power, 1994). Pendergast (1989) has argued that some of the St-Lawrence Iroquois retreated to the Missisquoi Valley in Vermont (60–80 km from our site) during AD 1550–1580. In AD 1609, Champlain observed extensive maize fields on the eastern shore of Lake Champlain (Calloway, 1994). During the French Colonial Regime, there were frequent wars between the Abenakis (with their French allies) and the Haudenosaunee (with their English allies), but the Missisquoi Abenaki remained in northern Vermont/southern Québec just to the southwest of our site with their main village at Missisquoi at the mouth of the Missisquoi River (80 km away), continuing to farm maize (Calloway, 1994). There has been no archeological work done in the Mont-Orford area, but there are archeological sites in Vermont, in the Missisquoi Valley (located 40 km to the south) (Haviland and Power, 1994). There was no permanent French settlement in the Mont-Orford region at this time. Hence, if our chronology is correct, the initial Poaceae/*Ambrosia* rise could be due to Missisquoi Abenaki/St-Lawrence Iroquois agriculture.

Nouvelle France fell in AD 1760 to the British. In the ensuing peace, European settlement began to increase in the Eastern Townships of southern Québec where our site is located. The second *Ambrosia* rise, beginning ~AD 1770, is more characteristic of the classic *Ambrosia* rises captured in southern Québec studies marking the onset of extensive European agriculture (Lafontaine-Boyer and Gajewski, 2014; Lavoie et al., 2007; Muller and Richard, 2001; Paquette and Gajewski, 2013). *Ambrosia* is a weedy herb that thrives with deforestation, disturbance and farming, particularly European-style cereal farming. Although native to eastern North America, *Ambrosia* expanded greatly with non-Indigenous settlement and provides a reliable marker for European settlement (e.g. Brugam, 1978; Grimm, 1983, 2001). The classic *Ambrosia* rise at ~AD 1770 at Étang Fer-de-Lance is within the time-frame of the *Ambrosia* rise of Muller and Richard (2001) in the

Monteregian Hills northwest of Mont-Orford. Muller and Richard (2001), using a 15-core study, determined that the regional *Ambrosia* rise occurred between AD 1750 and 1800 as the result of European-caused deforestation and agriculture. Further north, Lafontaine-Boyer and Gajewski (2014) and Paquette and Gajewski (2013) found an *Ambrosia* rise between AD 1810 and 1860 at Lacs Noir and Brulé, corresponding to settlement in that region. In the Eastern Townships of Québec, settlement by Europeans began in the late 1700s with the Constitutional Act of 1791 of the Parliament of Great Britain, which reformed the province's government (St-Onge and Will, 2019). In this second *Ambrosia* rise, our record possibly captures the beginning of the United Empire Loyalist (i.e. refugees from the United States) settlement in the Mont-Orford region at Magog in AD 1776 (Figure 1).

Further European settler impacts over the last 200 years

In addition to increasing pioneering weedy taxa with high light demands, that is, *Ambrosia* and Poaceae, the land disturbance of European settlers in the region has had lasting impacts on forest composition. Over the last 200 years, Étang Fer-de-Lance shows a significant increase in *Acer* spp. pollen, particularly *A. rubrum*, *A. pensylvanicum* and *A. saccharum*, following the second rise of *Ambrosia* (Supplemental Figure 4). Using early European land settlement surveys to infer early forest inventories, Danneyrolles et al. (2019) show how agricultural clearing, logging, and anthropogenic fires have influenced forest dynamics in southern Québec by benefiting disturbance-adapted, early-successional, short-lived, and fast-growing tree species, such as *Acer* spp. Gauvin and Bouchard (1983) also identified *Acer* spp. as a marker of forestry in their vegetational survey of the Parc national du Mont-Orford, finding that sectors disturbed by forestry had been reclaimed by successional communities of *Acer*, *Betula*, and *Populus* species. These anthropogenic disturbances and increases of *Acer* and other early successional species came at the expense of long-lived late-successional taxa, such as *T. canadensis* and *F. grandifolia* (Bouchard et al., 1989; Boucher et al., 2009; Danneyrolles et al., 2019; Simard and Bouchard, 1996). The Étang Fer-de-Lance pollen record detects the arboreal species shifts described by these forest inventory and notary deed studies, as early- and mid-successional *Acer* spp. percentages increase at the *Ambrosia* rise peak with concomitant declines in late-successional *T. canadensis* and *F. grandifolia* percentages. To the best of our knowledge, this study is the first in southern Québec to link sedimentary pollen results to those from early settlement forest inventory studies, demonstrating that high-temporal and high-taxonomic resolution palynology can be used to reconstruct sub-centennial forest history on a longer time-scale than that possible using historical records in this region.

Pre-Contact and European fire record

Four significant CHAR peaks denoting local fires mark our 2300-year fire record from Étang Fer-de-Lance (Figure 3). The CHAR peaks at ~AD 670, ~AD 1090, and ~AD 1660 are possibly non-anthropogenic in origin as they precede European settlement of the region. However, they could have been set by Indigenous people, although no present-day nearby Indigenous nation has recorded extensive use of fire in their oral histories. Pollen percentages and influxes do not show any substantial changes in forest composition due to these fires (Figure 3 and Supplemental Figure 5). The most recent significant fire event at ~AD 1800 corresponds to the early European settlement of the Eastern Townships region. As the initial settlement of the city of Sherbrooke begun in the early 1800s (Figure 1), the CHAR peak at ~AD 1800 matches the period when European

land clearance would have been beginning (Eastern Townships Resource Centre, 2017).

If we assume that the first three fires were non-anthropogenically ignited (excluding the ~AD 1800 European CHAR peak), the mean fire return interval of 515 years is typical of the hardwood forests of southeastern Canada, known for a relatively moist climate and less fuel accumulation during the late Holocene (Blarquez et al., 2018). The accuracy of this calculation should be treated with caution; however, given the relatively short time-span of the core and the small number of fires. Comparatively, in the Gatineau region of drier southwestern Québec, Blarquez et al. (2018), recorded a mean fire return interval of 301 ± 201 years for the last 1500 years at Folly Bog. Stager et al. (2016) found a mean fire return interval of 210 years at Wolf Lake in the Adirondacks (Figure 1). Lavoie et al. (2013) found four major charcoal peaks above background in the most recent 2600 years from a peat bog core at Covey Hill (45°00'29"N, 73°49'36"W – 130 km to the west, located in the sugar maple-bitternut hickory forest domain), which corresponds well to Étang Fer-de-Lance. Payette et al. (2015, 2016) dated soil microcharcoal pieces and found that fire has been a part of *T. canadensis* and *Acer* stands in the eastern sugar maple-basswood forest domain throughout the last 2000 years. We conclude from our pollen and charcoal records that while fires are a re-occurring part of the Mont-Orford forest landscape, this fire regime likely did not play a major role in vegetation dynamics prior to significant land clearing by European settlers. To the best of our knowledge, this is the first lacustrine microcharcoal study from the eastern sugar maple-basswood domain of the hardwood forest subzone of Northern Temperate Forest (Ressources Naturelles Québec, 2003).

Climate reconstructions

We converted the Étang Fer-de-Lance pollen data into temperature and precipitation reconstructions and compared the climate signal from our site with those from broader regional paleoclimate syntheses (Ladd et al., 2018; Marlon et al., 2017; Shuman et al., 2018) and other nearby high-resolution, terrestrial sediment-based climate reconstructions within a ~350 km radius (Figures 1, 6, and 7). We assume that if our reconstructions are similar to the above, then the forest changes in the Étang Fer-de-Lance pollen record are most likely caused by regional climate change, and not internal drivers (e.g. succession). We did not include tree-ring-based climate reconstructions in our local comparison set. Although annually resolved, they do not capture centennial-scale climate variability well here because of the aggressive detrending methods dendro-climatologists must use to remove stand dynamics in closed-canopy northeastern forests (e.g. Tardif et al., 2001).

The Étang Fer-de-Lance summer temperature reconstruction matches the coherent cooling pattern over the past 2000 years found in the synthesis paper of Marlon et al. (2017) which covers the northeastern United States. Focusing more locally, our summer temperature reconstruction also closely corresponds to pollen-based reconstructions from Lacs Noir and Brulé in the Ottawa River Valley 250 km to the west, with a warmer MCA than the subsequent LIA with a transition occurring between AD 1400–1500 at all three sites (Lafontaine-Boyer and Gajewski, 2014; Paquette and Gajewski, 2013) (Figure 6). Similarly, Gajewski (1988) found a shift from a warmer MCA to a colder LIA at ~AD 1450–1500 at Conroy Lake and Basin Pond in Maine also using pollen-based reconstructions. These two latter sites, together with his pollen-based Clear Pond in New York, also show a generally warmer first millennium AD than the MCA like Étang Fer-de-Lance. Hence, our temperature reconstruction follows the coherent broad regional temperature decline, suggesting that the shifts in forest composition at Étang Fer-de-Lance are being driven in part by this regional cooling.

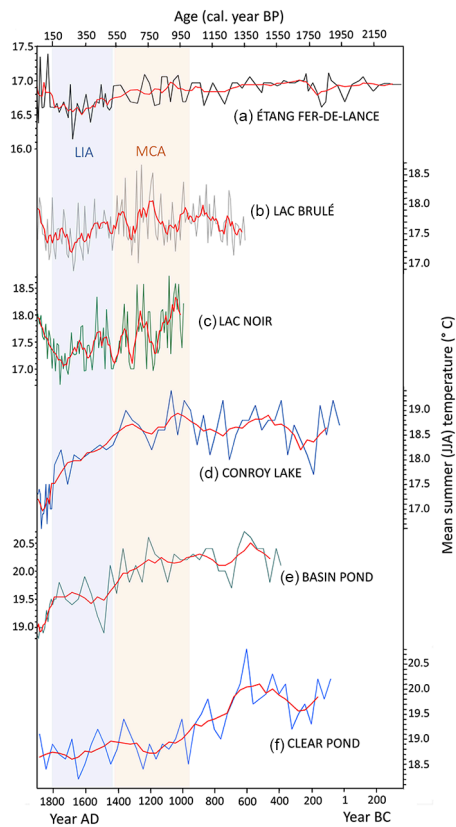


Figure 6. Mean summer (JJA) temperature summary of high-resolution and well-dated sedimentary sites within 350 km of Étang Fer-de-Lance: (a) this study, (b) Lac Brulé (Lafontaine-Boyer and Gajewski, 2014), (c) Lac Noir (Paquette and Gajewski, 2013), (d) Conroy Lake (Gajewski, 1988), (e) Basin Pond (Gajewski, 1988), and (f) Clear Pond (Gajewski, 1988).

Additionally, the Étang Fer-de-Lance mean annual precipitation reconstruction matches the coherent wetting pattern over the past 2000 years for northern New England described in the syntheses of Ladd et al. (2018), Marlon et al. (2017), and Shuman et al. (2018) (Figure 7), that is a wet LIA relative to the MCA, which is then wetter relative to the first millennium AD. Examining the local high-resolution reconstructions, the annual precipitation reconstruction from Conroy Lake, Maine, shows this wetting trend over the past two millennia (Gajewski, 1988), as does the water-table depth reconstruction from testate amoebae from Sidney Bog (Clifford and Booth, 2013) (Figures 1 and 7). Clear Pond, New York, shows little difference in moisture between the LIA and MCA, but the MCA is wetter relative to the first millennium AD (Gajewski, 1988). However, this wetting precipitation trend is less coherent in northern New England than the cooling temperature one is. There are records that show opposite or mixed trends because precipitation, both as rain and snow, is more heterogeneous over relatively smaller spatial scales than temperature (Shuman et al., 2018). The annual precipitation of Basin Pond, Maine, shows a drier LIA relative to the MCA and no substantial difference in moisture availability between the MCA and the first millennium AD (Gajewski, 1988). The planktonic and tycho planktonic diatom percentage record from Wolf Lake in the central Adirondacks shows a wetter LIA relative to the MCA, but the first millennium AD was also wet (Stager et al., 2016). In summary, our precipitation reconstruction follows the general northern New England pattern, suggesting that the shifts in forest composition at Étang Fer-de-Lance are also being driven in part by regional wetting, as well as by the regional cooling. Hence, together the late Holocene cooling and wetting trends in the broadly defined northern New England region

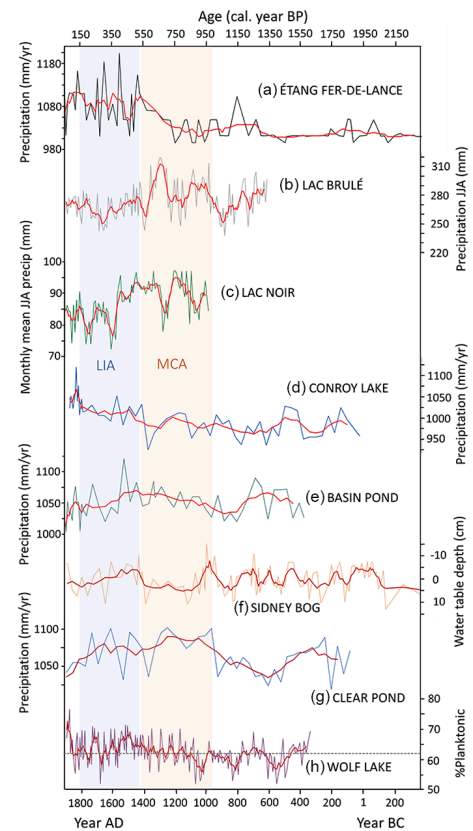


Figure 7. Precipitation summary of high-resolution and well-dated sedimentary sites within 350 km of Étang Fer-de-Lance: (a) annual precipitation from this study, (b) Lac Brulé JJA precipitation (Lafontaine-Boyer and Gajewski, 2014), (c) Lac Noir monthly mean JJA precipitation (Paquette and Gajewski, 2013), (d) Conroy Lake annual precipitation (Gajewski, 1988), (e) Basin Pond annual precipitation (Gajewski, 1988), (f) Sidney Bog water-table depth reconstruction residuals, with more negative residuals meaning wetter conditions (Clifford and Booth, 2013), (g) Clear Pond annual precipitation (Gajewski, 1988), and (h) Wolf Lake combined percentages of planktonic and tycho planktonic diatoms, with higher values representing greater precipitation in the watershed (Stager et al., 2016). Horizontal dotted line at 62% designates mean prior to AD 1860.

appear to be driving the forest composition changes seen at Étang Fer-de-Lance.

In their pollen-based synthesis, Ladd et al. (2018) found an opposing drying trend in the continental interior over the last 1600 years. Following this more continental pattern, the summer precipitation reconstructions of Lacs Noir and Brulé in the Ottawa River Valley show a drier LIA relative to the MCA even though they are relatively close to our site; hence there is no discordance here with our results (Lafontaine-Boyer and Gajewski, 2014; Paquette and Gajewski, 2013).

A number of caveats must be mentioned with respect to the calculations of the Étang Fer-de-Lance climate reconstructions. A serious issue in doing climate reconstructions based upon modern pollen-climate training sets is the fact that human-caused landscape disturbance is so great in many regions of the world (certainly in southern Québec) that vegetation no longer reflects climate in the same way that it used to prior to this major disturbance (Kujawa et al., 2016; St-Jacques et al., 2008b, 2015). Hence, when we use transfer functions built using modern pollen-climate training sets to infer the past climates of more pristine landscapes, there are inevitable errors that can be severe, including substantial climate signal flattening and underestimation, and bias (St-Jacques et al., 2008b, 2015). A further source of loss of sensitivity in our reconstructions arises from having to merge all *Picea* taxa together,

even though they have different climate optima (Thompson et al., 2015) because of the low taxonomic resolution used by earlier researchers whose compiled results comprise the pollen training set (Whitmore et al., 2005). An additional caveat arises from the fact that 12 out of the 14 20th-century Étang Fer-de-Lance samples are shown to have close analogs in the training set even though the independent historical record documents the heavy anthropogenic regional landscape alteration (Figure 5). Hence, common definitions of good analogs in training sets used to assess reconstruction reliability can be problematic (Simpson, 2012). However, even though there are problems with the absolute values of our reconstructions, they are trustworthy enough to compare to the general trends found in regional syntheses (e.g. Ladd et al., 2018; Marlon et al., 2017; Shuman et al., 2018).

Conclusions

In this study, we show how the changing climate of the first millennium AD (including the Dark Ages Cold Period), the MCA and the LIA affected the forest composition and pollen productivity at Étang Fer-de-Lance in the sugar maple-basswood domain of the Northern Temperate Forest of southeastern Québec. We show how high-resolution (bidecadal) pollen analysis is able to detect forest dynamics due to climate change in this region, where it has been speculated based on low-resolution pollen analysis that the forests were unresponsive to climate variability over the past 2000 years. Further work could be done examining the effects of the climate changes of the fairly variable first millennium AD, that is, the Roman Warm Period, the Dark Ages Cold Period and the MCA, on southeastern Québec forest composition from a core from a lake with a better age-depth model for this time period. Our study also demonstrates a complex pattern of anthropogenic vegetation modification since AD 1500 from possible Indigenous effects on the landscape to the severe landscape changes caused by European settlement. This recent human disturbance of the vegetation could also be fruitfully explored further using high-resolution sediment cores from other lakes in the region to better understand recent regional prehistory and history.

Acknowledgements

We thank the Parc national du Mont-Orford for their collaboration and coring permission. We also thank Duane Noel, Zach Masson and Fanny Lashcari for fieldwork assistance; Tanya O'Reilly for laboratory assistance; and Michelle Garneau, Olivier Blarquez, Pierre Richard, and two anonymous reviewers whose comments greatly improved this manuscript.

Funding

The author(s) disclosed receipt of the following financial support for the research, authorship, and/or publication of this article: This work was supported by a Natural Sciences and Engineering Research Council (NSERC) Discovery Grant 41795-2017 and a *Fonds de recherche du Québec – Nature et technologies (FRQNT) Nouveaux chercheurs* Grant to J-MS-J and funding from the Canada Foundation for Innovation John R. Evans Leaders Fund, the Canada Research Chairs Program, and Bishop's University Professional Development Fund to MP.

ORCID iD

Jeannine-Marie St-Jacques  <https://orcid.org/0000-0002-4416-2293>

Data availability

The pollen and microcharcoal data is archived at Neotoma (<https://www.neotomadb.org/data/category/explorer>) and the climate

reconstructions are archived at the NOAA Paleoclimatology site (<https://www.ncdc.noaa.gov/data-access/paleoclimatology-data>).

Supplemental material

Supplemental material for this article is available online.

References

- Bassett J, Crompton C and Parmelee J (1978) *An Atlas of Airborne Pollen Grains and Common Fungus Spores of Canada*. Ottawa: Biosystematics Research Institute, Agriculture Canada.
- Benninghoff WS (1962) Calculation of pollen and spore density in sediments by addition of exotic pollen in known quantities. *Pollen et Spores* 4: 332–333.
- Berglund B (ed.) (1986) *Handbook of Holocene Palaeoecology and Palaeohydrology*. Caldwell, NJ: Blackburn Press.
- Blaauw M and Christen JA (2011) Flexible paleoclimate age-depth models using an autoregressive gamma process. *Bayesian Analysis* 6: 457–474.
- Blarquez O, Talbot J, Paillard L et al. (2018) Late Holocene influence of societies on the fire regime in southern Québec temperate forests. *Quaternary Science Reviews* 180: 63–74.
- Bonny AP (1972) A method for determining absolute pollen frequencies in lake sediments. *New Phytology* 71: 393–405.
- Bouchard A, Dyrda S, Bergeron Y et al. (1989) The use of notary deeds to estimate the changes in the composition of the 19th century forests, in Haut-Saint-Laurent, Quebec. *Canadian Journal of Forest Research* 19: 1146–1150.
- Boucher Y, Arseneault D and Sirois L (2009) La forêt préindustrielle du Bas-Saint-Laurent et sa transformation (1820–2000): Implications pour l'aménagement écosystémique. *Naturaliste canadien* 133: 60–69.
- Brugam RB (1978) Pollen indicators of land-use change in southern Connecticut. *Quaternary Research* 9: 349–362.
- Calloway CA (1994) *The Western Abenakis of Vermont, 1600–1800: War, Migration and the Survival of an Indian People*. Oklahoma: University of Oklahoma Press.
- Campbell ID and McAndrews JH (1993) Forest disequilibrium caused by rapid Little Ice Age cooling. *Nature* 366: 336–338.
- Carcaillet C and Richard PJH (2000) Holocene changes in seasonal precipitation highlighted by fire incidence in eastern Canada. *Climate Dynamics* 16: 549–559.
- Clark JS and Royall PD (1996) Local and regional sediment charcoal evidence for fire regimes in presettlement North-Eastern North America. *Journal of Ecology* 84: 365–382.
- Clifford MJ and Booth RK (2013) Increased probability of fire during late Holocene droughts in northern New England. *Climate Change* 119: 693–704.
- Danneyyrolles V, Dupuis S, Fortin G et al. (2019) Stronger influence of anthropogenic disturbance than climate change on century-scale compositional changes in northern forests. *Nature Communications* 10(1): 1–7.
- Davis RB, Bradstreet TE, Stuckenrath R Jr et al. (1975) Vegetation and associated environments during the past 14,000 years near Moulton Pond, Maine. *Quaternary Research* 5: 435–465.
- Dechêne L (1992) *Habitants and Merchants in Seventeenth Century Montréal*. London: McGill-Queen's University Press, Montréal and Kingston.
- Eastern Townships Resource Centre (2017) Hyatt family fonds. Available at: www.townshipsarchives.ca/downloads/hyatt-family-fonds.pdf (accessed 10 May 2020).
- Faegri K and Iversen J (1989) *Textbook of Pollen Analysis*. 4th ed. Chichester: John Wiley & Sons.
- Gajewski K (1987) Climatic impacts on the vegetation of eastern North America during the past 2000 years. *Vegetatio* 68: 179–190.

- Gajewski K (1988) Late Holocene climate changes for eastern North America estimated from pollen data. *Quaternary Research* 29: 255–262.
- Gajewski K, Swain AM and Peterson GM (1987) Late Holocene pollen stratigraphy in four northeastern United States lakes. *Géographie physique et quaternaire* 3: 377–386.
- Gauvin C and Bouchard A (1983) La végétation forestière du parc du Mont-Orford, Québec. *Canadian Journal of Botany* 61(5): 1522–47.
- Ghaleb B (2009) Overview of the methods for the measurement and interpretation of short-lived radioisotopes and their limits. In: *IOP conference series: Earth and environmental science*, vol. 5, Faro, Portugal, 25–29 February 2008, p. 012007. IOP Science.
- Government of Canada (2019) Canadian Climate Normals 1981–2010 Station Data, MAGOG. Available at: https://climate.weather.gc.ca/climate_normals/results_1981_2010_e.html?stnID=5401&autofwd=1 (accessed 31 January 2020).
- Grimm EC (1983) Chronology and dynamics of vegetation change in the prairie-woodland region of southern Minnesota, USA. *New Phytologist* 93: 311–350.
- Grimm EC (2001) Trends and palaeoecological problems in the vegetation and climate history of the northern Great Plains, USA. *Proceedings of the Royal Irish Academy* 101B: 47–64.
- Grochocki KK, Lane CS and Stager JC (2019) An 1800-year record of environmental change from the southern Adirondack Mountains, New York (USA). *Journal of Paleolimnology* 62(3): 301–134.
- Haudenosaunee Confederacy (2020) Food and hunting. Available at: <https://www.haudenosauneeconfederacy.com/historical-life-as-a-haudenosaunee/food-and-hunting/> (accessed 7 May 2020).
- Hausmann S, Larocque-Tobler I, Richard PJH et al. (2011) Diatom-inferred wind activity at Lac du Sommet, southern Québec, Canada: A multiproxy paleoclimate reconstruction based on diatoms, chironomids and pollen for the past 9500 years. *Holocene* 21: 925–938.
- Haviland WA and Power MW (1994) *The Original Vermonters: Native Inhabitants, Past and Present*. Lebanon, NH: University Press of New England.
- Heiri O, Lotter AF and Lemcke G (2001) Loss on ignition as a method for estimating organic and carbonate content in sediments: Reproducibility and comparability of results. *Journal of Paleolimnology* 25: 101–110.
- Helama S, Jones PD and Briffa KR (2017) Dark Ages Cold Period: A literature review and directions for future research. *Holocene* 10: 1600–1606.
- Higuera P (2009) *CharAnalysis 0.9: Diagnostic and Analytical Tools for Sediment-Charcoal Analysis* 27. Bozeman, MT: Montana State University
- Higuera PE, Brubaker LB, Anderson PM et al. (2009) Vegetation mediated the impacts of postglacial climatic change on fire regimes in the south-central Brooks Range, Alaska. *Ecological Monographs* 79: 201–219.
- Houle D, Richard PJH, Ndzangou SO et al. (2012) Compositional vegetation changes and increased red spruce abundance during the Little Ice Age in a sugar maple forest of North-Eastern North America. *Plant Ecology* 213(6): 1027–1035.
- Juggins S (2007) *C2 Version 1.5 User Guide. Software for Ecological and Palaeoecological Data Analysis and Visualisation*. Newcastle upon Tyne: Newcastle University, p. 73.
- Juggins S (2019) Package “Rioja”: Analysis of Quaternary science data (version 0.9-21). Available at: <https://cran.r-project.org/web/packages/rioja/index.html> (accessed 4 February 2021).
- Kaufman DS, McKay N, Routson C et al. (2020) A global database of Holocene paleo-temperature records. *Nature Scientific Data* 7: 115.
- Kujawa ER, Goring S, Dawson A et al. (2016) The effect of land cover change on pollen-vegetation relationships in the American Midwest. *Anthropocene* 15: 60–71.
- LacCore (2016) *Pollen preparation procedure*. University of Minnesota. SOP Collection. Available at: <http://lrc.geo.umn.edu/laccore/assets/pdf/sops/pollen.pdf> (accessed 16 July 2018).
- Ladd M, Viau AE, Way RG et al. (2018) Variations in precipitation in North America during the past 2000 years. *Holocene* 28: 667–675.
- Lafontaine-Boyer K and Gajewski K (2014) Vegetation dynamics in relation to late Holocene climate variability and disturbance, Outaouais, Québec, Canada. *Holocene* 24(11): 1515–1526.
- Lavoie C, Jodoin Y and De Merlis AG (2007) How did common ragweed (*Ambrosia artemisiifolia* L.) spread in Québec? A historical analysis using herbarium records. *Journal of Biogeography* 34: 1751–1761.
- Lavoie M, Pellerin S and Larocque M (2013) Examining the role of allogeneous and autogeneous factors in the long-term dynamics of a temperate headwater peatland (southern Québec, Canada). *Palaeogeography, Palaeoclimatology, Palaeoecology* 386: 336–348.
- Lavoie M and Richard PJH (2000) Postglacial water-level changes of a small lake in southern Québec, Canada. *Holocene* 10(5): 621–634.
- Lavoie M and Richard PJH (2017) The 8200-year vegetation history of an urban woodland as reconstructed from pollen and plant remains. *Botany* 95(2): 163–172.
- Lindbladh M, Jacobson GL and Schauffler M (2003) The post-glacial history of three *Picea* species in New England, USA. *Quaternary Research* 59(1): 61–69.
- Loisel J and Gameau M (2010) Late Holocene paleoecohydrology and carbon accumulation estimates from two boreal peat bogs in eastern Canada: Potential and limits of multi-proxy archives. *Palaeogeography, Palaeoclimatology, Palaeoecology* 291: 493–533.
- Marlon JR, Pedersen N, Nolan C et al. (2017) Climatic history of the northeastern United States during the past 3000 years. *Climate of the Past* 13, 1355–1379.
- McAndrews JH, Berti A and Norris G (1973) *Key to the Quaternary Pollen and Spores of the Great Lakes Region*, Toronto, Ontario: Royal Ontario Museum.
- Moore PD, Webb JA and Collinson ME (1991) *Pollen Analysis*, 2nd edn. Oxford: Blackwell.
- Mott RJ (1977) Late-Pleistocene and Holocene palynology in southeastern Québec. *Géographie physique et quaternaire* 31(1–2): 139.
- Muller SD and Richard PJH (2001) Post-glacial vegetation migration in conterminous Montréal lowlands, southern Québec. *Journal of Biogeography* 28: 1169–1193.
- Muller SD, Richard PJH, Guiot J et al. (2003) Postglacial climate in the St. Lawrence lowlands, southern Québec: Pollen and lake-level evidence. *Palaeogeography, Palaeoclimatology, Palaeoecology* 193(1): 51–72.
- Nolan CJ (2019) *Using co-located lake and bog records to improve inferences on late Quaternary climate and ecology*. PhD Thesis, University of Arizona, Arizona.
- Oswald WW, Anderson PM, Brown TA et al. (2005) Effects of sample mass and macrofossil type on radiocarbon dating of arctic and boreal lake sediments. *Holocene* 15(5): 758–767.
- Oswald WW, Foster DR, Shuman BN et al. (2018) Subregional variability in the response of New England vegetation to post-glacial climate change. *Journal of Biogeography* 45: 2375–2388.
- Overpeck JT, Webb T III and Prentice IC (1985) Quantitative interpretation of fossil pollen spectra: Dissimilarity coefficients and the method of modern analogs. *Quaternary Research* 23: 87–108.

- Paquette N and Gajewski K (2013) Climatic change causes abrupt changes in forest composition, inferred from a high-resolution pollen record, southwestern Quebec, Canada. *Quaternary Science Reviews* 75: 169–180.
- Payette S, Pilon V, Couillard PL et al. (2015) Holocene dynamics of an eastern hemlock (*Tsuga canadensis*) forest site at the northern range of the species limit. *Holocene* 25: 1246–1256.
- Payette S, Pilon V, Couillard PL et al. (2016) Long-term fire history of maple (*Acer*) forest sites in the central St. Lawrence Lowland, Quebec. *Canadian Journal of Forest Research* 46(6): 822–831. DOI: 10.1139/cjfr-2015-0305.
- Pellerin S, Larocque M and Lavoie M (2007) *Rôle hydrologique et écologique régional de la tourbière de Covey Hill*. Research report presented to the EJLB Foundation. DOI: 10.13140/RG.2.1.1764.5040.
- Pendergast JF (1989) Native encounters with Europeans in the region now known as Vermont in the 16th century. In: *Paper presented at the Vermont Historical Society Conference*, Vermont and Canada, Regional Ties that Bind, Montpelier, Vermont.
- Ramsey CB (2009) Bayesian analysis of radiocarbon dates. *Radiocarbon* 51: 337–360.
- Reimer PJ, Bard E, Bayliss A et al. (2013) IntCal13 and MARINE13 radiocarbon age calibration curves 0–50000 years cal BP. *Radiocarbon* 55(4): 1869–1887.
- Ressources Naturelles Québec (2003) Vegetation zones and bioclimatic domains in Québec. Available at: <http://mern.gouv.qc.ca/english/publications/forest/publications/zone-a.pdf> (accessed 7 March 2019).
- Richard PJH (1970) Atlas pollinique des arbres et de quelques arbustes indigènes du Québec. *Naturaliste Canadien* 97(1): 1–306.
- Richard PJH (1975) Contribution à l'histoire postglaciaire de la végétation dans les Cantons-de-l'Est: étude des sites de Weedon et Albion. *Cahiers de géographie du Québec* 19: 267. DOI: 10.7202/021257ar.
- Richard PJH (1978) Histoire tardiglaciaire et postglaciaire de la végétation au mont Shefford, Québec. *Géographie physique et quaternaire* 32(1): 81–93.
- Richard PJH (1994) Postglacial palaeophytogeography of the eastern St. Lawrence River watershed and the climatic signal of the pollen record. *Palaeogeography, Palaeoclimatology, Palaeoecology* 109: 137–161.
- Ruddiman WF (2008) *Earth's Climate: Past and Future*, 2nd edn. New York: W.H. Freeman and Company.
- Santer B, Wigley TML, Boyle JS et al. (2000) Statistical significance of trends and trend differences in layer-average atmospheric temperature time series. *Journal of Geophysical Research* 105: 7337–7356.
- Schauffler M and Jacobson GL (2002) Persistence of coastal spruce refugia during the Holocene in northern New England, USA, detected by stand-scale pollen stratigraphies. *Journal of Ecology* 90: 235–250.
- Shuman BN, Routson C, McKay N et al. (2018) Placing the Common Era in a Holocene context: Millennial-to-centennial patterns and trends in the hydroclimate of North America over the past 2000 years. *Climate of the Past* 14: 665–686.
- Simard H and Bouchard A (1996) The precolonial 19th century forest of the Upper St. Lawrence Region of Quebec: A record of its exploitation and transformation through notary deeds of wood sales. *Canadian Journal of Forest Research* 26: 1670–1676.
- Simpson GL (2012) Analogue methods in paleolimnology. In: Birks HJB, Lotter AF, Juggins S, et al. (eds) *Tracking Environmental Change Using Lake Sediments. Developments in Paleoenvironmental Research 5*, Dordrecht: Springer Netherlands, pp.495–522.
- Société des Établissements de Plein Air du Québec (2019) *Portrait of the Park: History of Parc National du Mont-Orford*. Available at: https://www.sepaq.com/pq/mor/decouvrir/portrait.dot?language_id=1 (accessed 16 February–25 May 2019).
- Sorgente D, Frignani M, Langone L et al. (1999) Chronology of marine sediment: Interpretation of activity-depth profiles of ²¹⁰Pb and other radioactive tracers. Part 1 (Technical Report No. 54). Bologna: Consiglio Nazionale Delle Ricerche Istituto per la Geologia Marina Bologna.
- Stager JC, Cumming BF, Laird KR et al. (2016) A 1600-year diatom record of hydroclimate variability from Wolf Lake, New York. *Holocene* 27: 246–257.
- St-Jacques JM, Cumming BF and Smol JP (2008a) A 900-year pollen-inferred temperature and effective moisture record from varved Lake Mina, west-central Minnesota, USA. *Quaternary Science Reviews* 27(7–8): 781–96.
- St-Jacques JM, Cumming BF and Smol JP (2008b) A pre-European settlement pollen-climate calibration set for Minnesota, USA: Developing tools for paleoclimatic reconstructions. *Journal of Biogeography* 35: 306–324.
- St-Jacques JM, Cumming BF, Sauchyn DJ et al. (2015) The bias and signal attenuation present in conventional pollen-based climate reconstructions as assessed by early climate data from Minnesota. *PLoS one* 10(1): e0113806. DOI: 10.1371/journal.pone.0113806.
- St-Onge A and Will F (2019) The settlement of the Eastern Townships by Loyalists: Myth or reality? Eastern Townships Resource Centre. Available at: http://www.etr.ca/wp-content/uploads/2019/04/Loyal_cahier_documentaire_ENG.pdf (accessed 6 May 2020).
- Tardif J, Brisson J and Bergeron Y (2001) Dendroclimatic analysis of *Acer saccharum*, *Fagus grandifolia*, and *Tsuga canadensis* from an old-growth forest, southwestern Quebec. *Canadian Journal of Forest Research* 31(9): 1491–1501.
- Thompson RS, Anderson KH, Pellier RT et al. (2015) *Atlas of relations between climatic parameters and distributions of important trees and shrubs in North America—revisions for all taxa from the United States and Canada and new taxa from the western United States*. U.S. Geological Survey Professional Paper 1650–G, DOI: 10.3133/pp1650G.
- Tremblay R (2006) *Les Iroquoiens du Saint-Laurent: peuple du maïs*. Montréal: Pointe-à-Callière : musée d'archéologie et d'histoire de Montréal.
- van Bellen S and ClimHuNor Project Members (2018) Proxy, historical, instrumental and model re-analysis climate records in the NW North Atlantic and adjacent Canada during the last 2 ka. In: *Joint Meeting of the Canadian and American Quaternary Associations – Crossing Borders in the Quaternary Abstracts*, Ottawa, Canada, 7–11 August 2018, p. 96. Available at: <https://www.quaternary2018.com/>
- van Bellen S and ClimHuNor Project Members (2020) A database of Holocene temperature records for north-eastern North America and the north-western Atlantic. *Geoscience Data Journal* 7: 38–43.
- Whitmore J, Gajewski K, Sawada M et al. (2005) Modern pollen data from North America and Greenland for multi-scale paleoenvironmental applications. *Quaternary Science Reviews* 24(16–17): 1828–1848.